Effect of Core Crystallization and Conformational Entropy on the Molecular Exchange Kinetics of Polymeric Micelles

Thomas Zinn,[†] Lutz Willner,[‡] Vitaliy Pipich,[¶] Dieter Richter,[§] and Reidar Lund[*,†]

Department of Chemistry, University of Oslo, Postboks 1033 Blindern, 0315 Oslo, Norway, Jülich Centre for Neutron Science JCNS and Institute for Complex Systems ICS, Forschungszentrum Jülich GmbH, 52425 Jülich, Germany, Jülich Centre for Neutron Science JCNS, Forschungszentrum Jülich GmbH, Outstation at MLZ, Lichtenbergstrasse 1 85747 Garching, Germany., and Jülich Centre for Neutron Science JCNS and Institute for Complex Systems ICS, Forschungszentrum Jülich GmbH, 52425 Jülich, Germany.

E-mail: reidar.lund@kjemi.uio.no

Abstract

Here we study the equilibrium molecular exchange kinetics of a systematic series of amphiphilic n-alkyl -poly(ethylene oxide) ($C_n - PEO$) micelles containing partly crystallized cores. Using differential scanning calorimetry (DSC), we determined the

[*]To whom correspondence should be addressed

[†]Department of Chemistry, University of Oslo, Postboks 1033 Blindern, 0315 Oslo, Norway

[‡]Jülich Centre for Neutron Science JCNS and Institute for Complex Systems ICS, Forschungszentrum Jülich GmbH, 52425 Jülich, Germany

[¶]Jülich Centre for Neutron Science JCNS, Forschungszentrum Jülich GmbH, Outstation at MLZ, Lichtenbergstrasse 1 85747 Garching, Germany.

[§]Jülich Centre for Neutron Science JCNS and Institute for Complex Systems ICS, Forschungszentrum Jülich GmbH, 52425 Jülich, Germany.

melting transition and extracted the enthalpy of fusion, ΔH_{fus}, of the n-alkyl chains inside the micellar core. Molecular exchange kinetics was measured below the melting point using a time-resolved small-angle neutron scattering technique (TR-SANS) based on mixing deuterated and proteated but otherwise identical micelles. Comparing both kinetic and thermodynamic data, we find that crystallinity within the micellar cores leads to significant enthalpic and the entropic contributions to the activation barrier for molecular exchange. While the former leads to an enhanced stability, the positive entropic gain favours the process. Interestingly, the entropic term contains an excess term beyond what is expected from the measured entropy of fusion. Based on calculations using the Rotational Isomeric State (RIS) model, we suggest that the excess entropy is due to the gain in conformational entropy upon releasing the chain from the confined state in the core. The study thus provides deep insight into the fundamental processes of micellar kinetics and which might be relevant also to other semi-crystalline soft matter and biological systems including lipid membranes.

Micellar aggregates attain their thermodynamic equilibrium via molecular exchange processes. Exchange kinetics in surfactant[1] or block copolymer micelles[2] has been well-understood as a thermally activated first order kinetic process characterized by a single activation energy, E_a associated with unfavorable contacts between the insoluble block and solvent.[3,4] Depending on the conformation of the insoluble block the surface free energy scales with the degree of polymerization N_{core}: $E_a \propto \gamma\, N_{\text{core}}^{\beta}$ [4,5] where γ is the interfacial tension. The scaling exponent, β, takes values between $2/3 \leq \beta \leq 1$ depending on the conformation of the chain during the expulsion process (collapsed or elongated, respectively). In this picture, the mobility of the chain segment within the core is usually considered to be equal to that in a melt.

Time-resolved small-angle neutron scattering (TR-SANS) technique in combination with a kinetic zero average contrast (KZAC) scheme is a powerful technique to monitor the molecular exchange processes in-situ.[2,6] In agreement with theory, the experiments showed that the chain exchange kinetics is essentially governed by single chain (unimer) exchange, which was also found for phosphoplipid bilayers.[7] The investigations revealed that the exchange kinetics in dilute solution is concentration independent, i.e. it is governed by the expulsion rate constant, which is critically dependent on the interfacial tension,[8] temperature,[9] molecular weight[10,11] and the core-block polydispersity.[10] In systems with large interfacial tensions (i.e. water), the exchange kinetics is "frozen".[9,12] The polydispersity gives rise to an extremely broad distribution of rate constants.[10] These experimental results suggest that the exchange process can be quite well understood as a non-cooperative, activated (self-) diffusion. For molecules with a tendency to crystallize, however, it is less clear how chain packing within the core would affect the molecular exchange processes.

Crystallization in micellar systems has indeed been shown to play a significant role in controlling and even driving the self-assembly process in many micellar[13–16] and other self-assembled systems.[17–19] The influence of crystallization on the exchange kinetics is less known. However it is generally believed that a crystalline core would increase the stability

of aggregates by increasing the residence time of the molecules within the micelles.[17,20] In a study by Tirrell and co-workers on PEGylated phospholipids,[17] it was found that the activation energy for monomer desorption contained a significant enthalpic contribution that could be associated with an ordered "glassy" n-alkyl, C_{18}, chain packing inside the micellar core.

In this work we systematically analyze the effect of crystallization on the molecular exchange in a series of very well defined poly(ethylene oxide) – mono – n-alkyl ether (C_n−PEO5) in water. In a previous study,[21] we showed that the micellar cores behave essentially as other nano-confined systems with a clear melting point depression, ΔT, that follows the Gibbs-Thomson equation, $\Delta T \propto \gamma/R_c$ where R_c is the core size and γ the surface tension. Here we show by combining TR-SANS and calorimetry that there is a significant contribution from crystallization that can be translated into an Eyring-like free energy of activation containing both an enthalpic and entropic part.

The equilibrium structural properties of the micelles in dilute solutions have been reported elsewhere.[22] In short, spherical star-like micelles are formed where the aggregation number increases from about 45 to 120 with increasing alkyl-length (see SI for details). To investigate the chain exchange kinetics, two individually prepared solutions of deuterated and proteated micelles in a H_2O/D_2O solvent mixture that matches the average contrast of the two differently labeled polymers are mixed in a 1:1 ratio and the time evolution of the scattered intensity, $I(t)$, is measured (see Si for more detailed description and .examples of TR-SANS curves) The extent of exchange can be expressed by a dimensionless relaxation function $R(t)$ given by:[2,8,9]

$$R(t) = \left[\frac{I(t) - I_\infty}{I_0 - I_\infty}\right]^{1/2} \tag{1}$$

here I_0 and I_∞ is the scattered intensity of the initial state $t = 0$ just after mixing, and the final state ($t \to \infty$) where all chains are equally redistributed among the micelles.[2]

As an example, Figure 1(a) shows the relaxation curves $R(t)$ for C_{28}−PEO5 micelles at 1% polymer volume fraction measured at different temperatures in a semi-logarithmic plot.

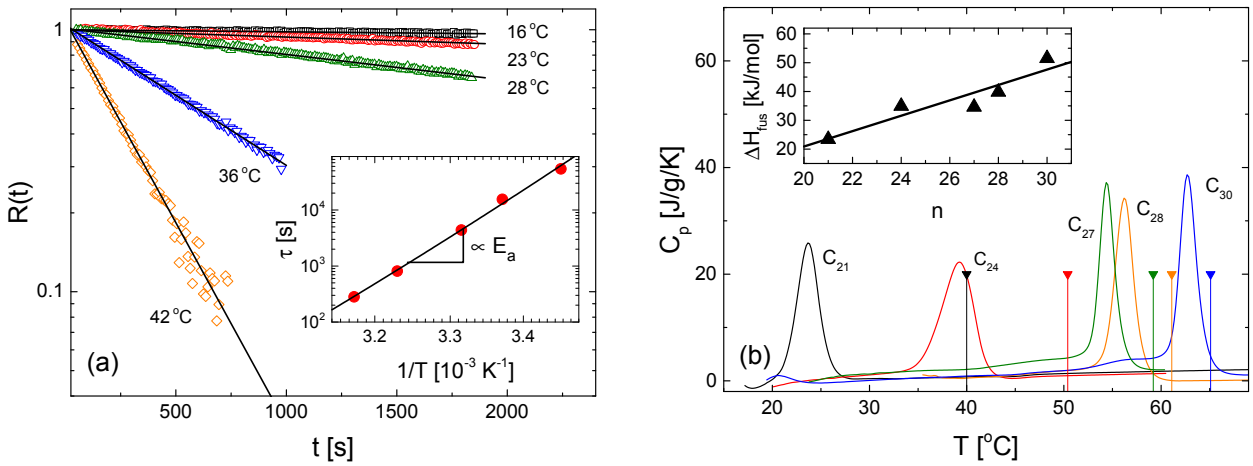

Figure 1: (a) Relaxation function of chain exchange kinetics of $C_{28}-$PEO5 micelles in aqueous solution (solid lines represent linear fit curves indicating a single-exponential time decay). The inset displays the Arrhenius plot of the temperature dependence of τ. (b) Nano-DSC thermograms of individual C_n-PEO5 micellar solutions as a function of n-alkyl chain size in units of specific heat capacity (heating rate: 2 K/min). The inset shows the determined enthalpy of fusion ΔH_{fus} as a function of the number of carbons n in the n-alkyl chain. The vertical lines correspond from left to right to the melting point for bulk $C_{21}H_{44}$ to $C_{30}H_{62}$.

At all temperatures we found the single exponential decay expected for the monodisperse n-alkyl block.[11] Thus, it is clear that there is an uniquely defined potential barrier also for crystallized cores. The inset of Figure 1(a) displays the temperature dependency of the extracted characteristic time constant τ in an Arrhenius representation: $\ln \tau$ vs. $1/T$. From this analysis, we obtain the activation energy, E_a, and the apparent fundamental time constant, τ_0, according to the Arrhenius equation:

$$\tau = \tau_0 \ \exp(E_a/RT) \tag{2}$$

Here τ_0 on a thermodynamic level is a system specific constant and is related to the time between each time the molecule "attempts" to overcome the energetic barrier. Both values E_a and τ_0 are listed in Table 1 for the different C_n-PEO5 polymers.

In a previous work we reported, based on densitometry, SAXS and calorimetry, that the spherical n-alkyl cores of the C_n-PEO5 micelles are partially crystalline.[21,22] The melting point of the confined hydrophobic tails, T_m, is shifted to lower temperatures compared to

Table 1: Kinetic and thermodynamic properties of the C_n−PEO5 micelles

n	T_m^0 [a] [K]	T_m [b] [K]	ΔH_{fus} [c] [kJ/mol]	ΔS_{fus} [d] [J/mol/K]	E_a [e] [kJ/mol]	τ_0 [f] [s]	$\tau_0^\dagger$ [g] [10^{-9} s]	ΔS_{ex} [h] [J/mol/K]
21	313	296	23	79	89	5.6×10^{-16}	3	50
24	323	312	35	112	124	2.4×10^{-20}	6	105
27	332	327	35	110	154	1.7×10^{-24}	9	191
28	334	329	40	121	160	8.5×10^{-25}	10	186
30	338	335	52	155	180	1.7×10^{-27}	14	207

[a] Melting point of pure n-alkanes; [b] Melting point n-alkyl in the micellar state (from DSC); [c] Enthalpy of fusion (from DSC); [d] Calculated entropy of fusion; [e] Activation energies extracted from Arrhenius plots (SANS); [f] Determined τ_0 from Arrhenius plots (SANS); [g] Estimated fundamental time constant $\tau_0^\dagger$ (MD-simulations); [h] Extracted conformational entropy.

pure n-alkanes (melting point depression) in bulk, T_m^0. It is important to note that all the kinetic experiments were carried out *below* the observed melting points (see Table 1) since chain exchange becomes immeasurable fast for TR-SANS at temperatures above T_m. The inset layer in Figure 1(b) shows the determined enthalpy of fusion ΔH_{fus} given by $\Delta H_{\text{fus}} = \int C_p \mathrm{d}T$, as a function of n-alkyl carbon atoms n. Within experimental error, we found that ΔH_{fus} increases linearly with n (see inset). This is also the case for the deduced activation energies E_a shown in Figure 2(a), although at this point it should mentioned that the range of n-alkanes is rather narrow such that a clear distinction between a $\sim n^{2/3}$ or n^1 scaling is difficult. Similar values of the activation energy were reported in ref.[23] for PEO polymers end-capped on both sides with shorter n-alkyl groups, e.g. for ($n = 18$): $E_a = 85\,\text{kJ/mol}$. In addition here the activation energies were found to scale linearly with n for $n \leq 18$.

Considering the melting of the partially crystalline core as an independent process, E_a is considered as the sum of two contributions: i) enthalpy of fusion ΔH_{fus} and, ii) the thermodynamic penalty arising from the creation of an additional surface area when the hydrophobic block is expelled from the core, E_a^0. $E_a^0 = E_a - \Delta H_{\text{fus}}$ is shown in Figure 2(a) (black squares). As mentioned above, the linear dependence suggests an elongated n-alkyl chain conformation where the whole chain is accessible for the solvent molecules ($\beta = 1$). The rather short chains thus do not have the conformational freedom to collapse to a compact

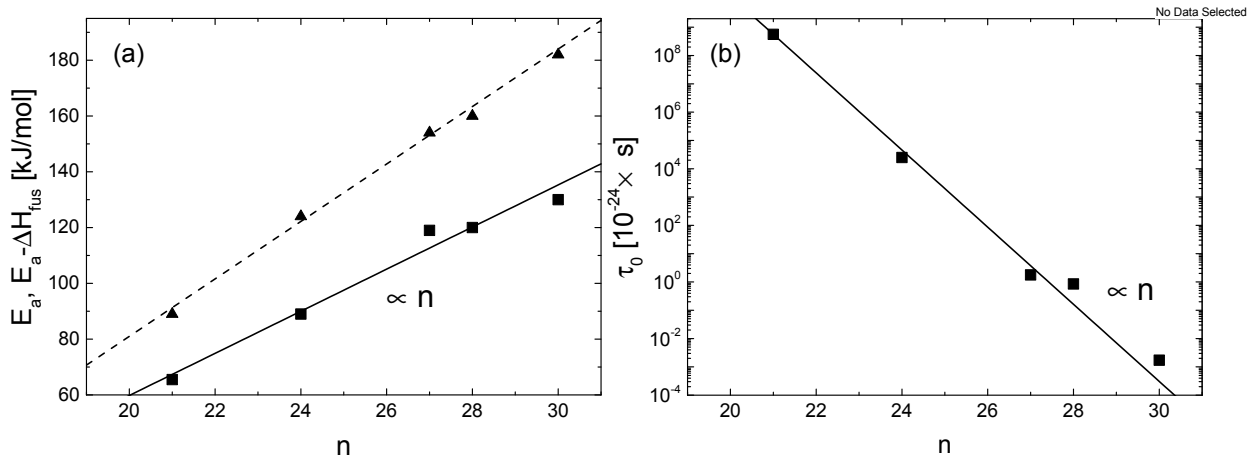

Figure 2: (a) Plot of E_a (triangles) and E_a corrected by $\Delta H_{\rm fus}$ (squares), respectively, vs. number of carbon atoms in the n-alkyl chain n. The dashed and straight lines represent linear regressions of the data: $y = 10.3\ x - 124$ (dashed line) and $y = 7.6\ x - 91$ (solid line) with correlation coefficient $R = 0.99$ and $R = 0.97$. (b) Dependence of $\ln \tau_0$ with n demonstrating a significant contribution of a conformational entropy, $\Delta S \sim n$.

globular state. Hence the kinetics cannot follow the predicted power law with $\beta = 2/3$ in agreement with an earlier study on the molecular exchange in cylindrical and spherical diblock copolymer micelles[5] and low-molecular weight surfactant micelles.[24]

The τ_0 values, which were extracted from the Arrhenius plots assume extremely small values ranging from 10^{-27} s to 10^{-16} s which obviously cannot be attributed to a fundamental time scale of diffusion ($\sim$ ns) suggesting a strong entropic contribution. In order to take this into account, we have to replace the activation energy E_a in Eq. (2) with the total activation free energy in a manner analogous to the classical theory of Eyring for chemical reactions, i.e. $E_a \to \Delta H^\ddagger - T\ \Delta S^\ddagger$.[25] Then Eq. (2) becomes

$$\tau = \tau_0^\dagger e^{-\Delta S^\ddagger/R}\ e^{\Delta H^\ddagger/RT} \tag{3}$$

with $\Delta H^\ddagger$ and $\Delta S^\ddagger$ the enthalpy and the entropy change, respectively, for the transfer of the hydrophobe from the core to the solvent rich micellar surface.[24] R in Eq. (3) is the universal gas constant. Within the present framework, it is clear that $\Delta H^\ddagger = E_a = E_a^0 + \Delta H_{\rm fus}$ where $\Delta H_{\rm fus}$ can be resolved by the DSC experiments. From Eq. (3) it is then becomes

obvious that τ_0 contains all entropic changes of the process. As demonstrated in Figure 2(b), $\log \tau_0 \propto \Delta S^{\ddagger} \propto n$, suggesting that the contribution may be due to conformational entropy which naturally scales with n.[26,27]

The fundamental time constant $\tau_0 = \tau_0^{\dagger} \exp[-\Delta S^{\ddagger}/R]$ can be intuitively understood as the characteristic diffusion time over a typical distance corresponding to the contour length of the chain ($L_c \approx (n-1) \cdot l_0$) such that $\tau_0^{\dagger} \propto L_c^2/(6D_{\text{self}})$ with D_{self} the self-diffusion constant of the n-alkyl group in the core. Using self-diffusion coefficients reported in a computer simulation study[28] for a series of n-alkanes we obtain an $\tau_0^{\dagger} \approx$ 3 - 14 ns which yields an average $\Delta S^{\ddagger}$ of the order of 130 J/K/mol to 360 J/K/mol. The change in entropy can be assumed to consist of two terms: $\Delta S^{\ddagger} = \Delta S_{\text{fus}} + \Delta S_{\text{ex}}$, where ΔS_{fus} is the entropy of fusion and ΔS_{ex} is an excess entropy. The former can be calculated from DSC measurements according to $\Delta S_{\text{fus}} = \Delta H_{\text{fus}}/T_m$ which yields values between 79 J/K/mol to 155 J/K/mol for the lowest and highest n, respectively (see Table 1). It becomes clear from Figure 3 that ΔS_{fus} increases linearly with n as found for pure n-alkanes.[29] Comparing the values of $\Delta S^{\ddagger}$ and ΔS_{fus} in Table 1, we see that there is an additional gain in entropy beyond what is expected from the melting within the core. This is not surprising as it is likely that the process provides an additional gain in entropy as the chain is able to adopt more possible orientations in a dissolved state compared to the "confined" state in the core.

The additional excess entropy ΔS_{ex} scales, as seen in Figure 3, within experimental uncertainties, almost linearly with n again suggesting an origin from conformational entropy. We may postulate that the conformational degree of freedom within the micellar core is very limited compared to the a free n-alkane chain in solution. The upper value for the entropic gain can be estimated by considering the rotational isomeric state (RIS) model[26] where the individual bonds can be assumed to adapt three states: trans, gauche$^+$ and gauche$^-$. A first and rather naive estimation can be obtained by assigning each conformation equally weighted, i.e. $S_{\text{conf}} \approx (n-2) \cdot R \ln 3$. However, a more realistic estimate is obtained by a full RIS calculation following an analytical formalism for the partition function for a

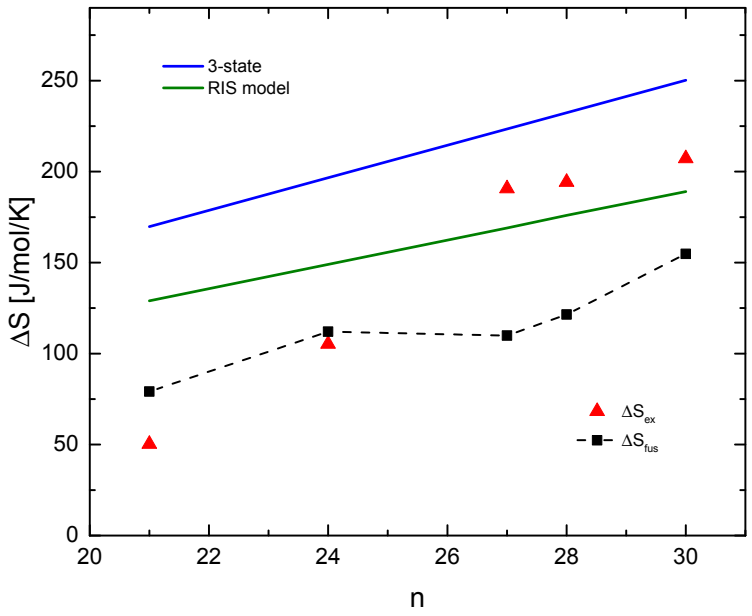

Figure 3: Contributions to the experimentally determined conformational entropy, $\Delta S^{\ddagger}$ and the individual components, ΔS_{fus} and ΔS_{ex} as a function of n-alkyl chain length. Comparison to theoretical considerations: a simple 3-state model (blue line), Florys' RIS-model n-alkanes (green line). The mismatch between $\Delta S^{\ddagger}$ and ΔS_{fus} suggests that the confinement imposed by the core restricts the conformational entropy of the n-alkane chains which is only fully recovered by releasing the chain into the solution.

chain molecule.[26] (see SI for detailed calculations). Since we know from the Nano-DSC measurements that the n-alkyl chains within the micellar cores are in crystalline state with a degree of crystallization of 50 to 80% depending on n. Crystallization requires a high degree of all-trans conformation for the necessary effective chain packing. Hence it it is justified to assume that the conformational entropy within the cores is approximately zero.

Calculating ΔS_{conf}, it is clear from Figure 3 that a relatively good correspondence with the estimated values for ΔS_{ex} is obtained. It should be mentioned that the expulsion rate also is expected to depend on the diffusion coefficient through the micellar corona. However, inclusion of this factor is likely to be a minor correction that will only slightly regulate the absolute value of the entropy. This will be subject for investigations in a future work. It should also be mentioned, that this work also suggests that there is a significant entropic penalty associated with the chain insertion process of micelles. Although this is not observed here, this might have significant implication to what time scale of the formation and

rearrangement of crystalline micelles.

In conclusion, by performing TR-SANS and DSC experiments in combination with a careful quantitative modeling on a systematic series of n-alkyl-PEOs we are able to unravel the basic mechanism and thermodynamic contributions to the chain expulsion process. In particular, we obtain a deeper understanding of the role of crystallinity on the dynamic behavior and stability of self-assembled systems, including drug -carriers. Although more work is needed, e.eg to unravel the exact dynamic motion in a crystallised core , this work provides essential insight which might be relevant also biological systems such as lipid membranes.[30]

Supplementary Information

Supporting Information available: synthesis, sample preparation, scattering experiments and RIS calculations. This material is available free of charge via the Internet at http://pubs.acs.org.

References

(1) Zana, R. *Dynamics of Surfactant Self-Assemblies: Micelles, Microemulsions, Vesicles and Lyotropic Phases*; Surfactant Science; Taylor & Francis, 2005.

(2) Lund, R.; Willner, L.; Richter, D. *Adv. Polym. Sci* **2013**, 51–158.

(3) Halperin, A.; Alexander, S. *Macromolecules* **1989**, *22*, 2403–2412.

(4) Halperin, A. *Macromolecules* **2011**, *44*, 5072–5074.

(5) Lund, R.; Willner, L.; Pipich, V.; Grillo, I.; Lindner, P.; Colmenero, J.; Richter, D. *Macromolecules* **2011**, *44*, 6145–6154.

(6) Willner, L.; Poppe, A.; Allgaier, J.; Monkenbusch, M.; Richter, D. *EPL* **2001**, *55*, 667–673.

(7) Nakano, M.; Fukuda, M.; Kudo, T.; Endo, H.; Handa, T. *Phys. Rev. Lett.* **2007**, *98*.

(8) Lund, R.; Willner, L.; Richter, D.; Dormidontova, E. E. *Macromolecules* **2006**, *39*, 4566–4575.

(9) Lund, R.; Willner, L.; Stellbrink, J.; Lindner, P.; Richter, D. *Phys. Rev. Lett.* **2006**, *96*, 068302.

(10) Choi, S.-H.; Lodge, T. P.; Bates, F. S. *Phys. Rev. Lett.* **2010**, *104*, 047802.

(11) Zinn, T.; Willner, L.; Lund, R.; Pipich, V.; Richter, D. *Soft Matter* **2011**, *8*, 623.

(12) Nicolai, T.; Colombani, O.; Chassenieux, C. *Soft Matter* **2010**, *6*, 3111.

(13) Richter, D.; Schneiders, D.; Monkenbusch, M.; Willner, L.; Fetters, L. J.; Huang, J. S.; Lin, M.; Mortensen, K.; Farago, B. *Macromolecules* **1997**, *30*, 1053–1068.

(14) Yin, L.; Lodge, T. P.; Hillmyer, M. A. *Macromolecules* **2012**, *45*, 9460–9467.

(15) Yin, L.; Hillmyer, M. A. **2011**, *44*, 3021–3028.

(16) Gilroy, J. B.; Gädt, T.; Whittell, G. R.; Chabanne, L.; Mitchels, J. M.; Richardson, R. M.; Winnik, M. A.; Manners, I. *Nature Chemistry* **2010**, *2*, 566–570.

(17) Kastantin, M.; Ananthanarayanan, B.; Karmali, P.; Ruoslahti, E.; Tirrell, M. *Langmuir* **2009**, *25*, 7279–7286.

(18) Loo, Y.-L.; Register, R. A.; Ryan, A. J. *Macromolecules* **2002**, *35*, 2365–2374.

(19) Fairclough, J. P. A.; Mai, S.-M.; Matsen, M. W.; Bras, W.; Messe, L.; Turner, S. C.; Gleeson, A. J.; Booth, C.; Hamley, I. W.; Ryan, A. J. *The Journal of Chemical Physics* **2001**, *114*, 5425.

(20) Dong, H.; Shu, J. Y.; Dube, N.; Ma, Y.; Tirrell, M. V.; Downing, K. H.; Xu, T. *JACS* **2012**, *134*, 11807–11814.

(21) Zinn, T.; Willner, L.; Lund, R. *Phys. Rev. Lett.* **2014**, *113*, 238305.

(22) Zinn, T.; Willner, L.; Lund, R.; Pipich, V.; Appavou, M.-S.; Richter, D. *Soft Matter* **2014**, *10*, 5212.

(23) Laflèche, F.; Nicolai, T.; Durand, D.; Gnanou, Y.; Taton, D. *Macromolecules* **2003**, *36*, 1341–1348.

(24) Aniansson, E. A. G.; Wall, S. N.; Almgren, M.; Hoffmann, H.; Kielmann, I.; Ulbricht, W.; Zana, R.; Lang, J.; Tondre, C. *J. Phys. Chem.* **1976**, *80*, 905–922.

(25) Eyring, H. *J. Chem. Phys.* **1935**, *3*, 107–115.

(26) Flory, P. J. *Statistical mechanics of chain molecules*; Interscience Publishers, 1969.

(27) Würflinger, A. *Colloid & Polymer Sci* **1984**, *262*, 115–118.

(28) Goo, G. H.; Sung, G. H.; Lee, S. H.; Chang, T. Y. *Bulletin of the Korean Chemical Society* **2002**, *23*, 1595–1603.

(29) Colussi, A. J.; Hoffmann, M. R.; Tang, Y. *Langmuir* **2000**, *16*, 5213–5217.

(30) Lipowsky, R.; Sackmann, E. *Structure and Dynamics of Membranes: I. From Cells to Vesicles / II. Generic and Specific Interactions*; Handbook of Biological Physics; Elsevier Science, 1995.

Graphical TOC Entry